Investigation of non-metallic inclusions in steel using hot stage Scanning electron microscope

Miikka Willman

Contents

1 Introduction

Non metallic inclusions in steel are very small non metallic particles trapped inside steel matrix that can have either positive or negative effects on properties of steel. Thus identifying and tracking the behaviour of these inclusions is vital for development of new manufacturing methods and refinement of old ones. Steel is the most used metal in the world and often used as a structural element in buildings, vehicles and tools etc. Therefore improving its properties, such as decreasing weight and improving strength, can have notable positive impact on performance and environmental effects in aforementioned use cases.

Non metallic inclusions (NMI) have been investigated by numerous different methods, each with their own strengths and weaknesses. Out of these approaches, scanning electron microscopy is the most commonly utilised in quick everyday investigation of inclusions. It is relatively affordable and versatile method and thus an attractive choice even for more demanding imaging tasks. In order to understand the behaviour of NMIs in the process of steel production and treatment in greater detail, a steel sample needs to be heated while being imaged. For this purpose, a scanning electron microscope (SEM) with heating stage (hot stage) is used in experiment covered by this thesis. A method that has not yet been tested for investigation of NMIs.

The first half of the thesis will shortly cover the principles of electron microscopy and the inner workings of hot stage scanning electron microscope (HT-SEM). Specifically the theory and methods presented here are focused towards analysing previously mentioned heated steel samples and identifying and analysing inclusions in those samples. The second half of the thesis is about analysing SEM data of these steel samples. The objective of this experiment is to see if there are any noticeable changes in either size or shape of multicomponent inclusions and if there is any diffusion between NMIs and the steel matrix. At the same time it will be evaluated if the hot stage SEM even is suitable for analysing inlcusions in steel. The data analyzed for this thesis is part of research carried out at University of Oulu [4, 5].

2 Non-metallic inclusions in steel

Non metallic inclusions are small non metallic particles trapped in the steel matrix that come in various sizes and compositions. In this thesis, the focus is going to be in NMIs sized from few microns to tens of microns as those are typical sizes to cause harm in steel manufacturing. Smaller inclusions than this tend to be harmless and larger inclusions are easier to get rid of without excessive effort. In terms of chemical composition, the inclusions can be, for example, different kinds of oxides, sulfides and nitrides (e.g. Al_2O_3, CaS, TiN).

As stated in the introduction, NMIs may introduce unwanted features to steel such as increased failures due to fatigue [2,3]. Thus knowing the behaviour of NMIs during various treatment processes of steel is important as that allows the refinement of manufacturing and treatment processes to minimize the negative properties or even get rid of harmful NMIs.

Investigating NMIs is not an easy task not only due to their generally small size, but also because they are embedded in the steel matrix. One approach is to use electrolytic extraction, where the steel matrix is dissolved away using electrolysis and the inclusions are collected for inspection. This will at least theoretically give easy access to all the inclusions in the sample and allow each inclusion to be the further investigated. The electrolysis

can however dissolve parts of the inclusions, so this is a partially destructive method. In addition, the behaviour of inclusions while inside the steel matrix cannot be investigated.

For a non-destructive option, an x-ray based method, like photoemission electron microscopy, can be used. These methods allow the inspection of inclusions in a steel sample and can provide both chemical and spatial properties of the inclusion. Downside of this approach is the cost and size of suitable x-ray source, like a synchrotron. For a more attainable solution, a scanning electron microscope produces similar results, although not without some limitations of its own. SEMs are relatively common and inexpensive instruments available in research institutes and also used in industry for quality control and research purposes. General working principles, advantages and disadvantages of SEM are discussed in later sections.

Traditional optical microscopes could also technically be used, at least when considering the maximum achievable resolution (≈ 200 nm). Unfortunately the restrictions that come with a visible light based method are too limiting for precise investigation and only more sophisticated forms of optical microscopy, like confocal laser scanning microscope (CLSM), have been successfully utilised in NMI investigation of any reasonable detail [6].

In addition to the actual imaging method, a method of heating should also be considered. As stated in the introduction, the target of this experiment is to observe possible changes in inclusions during heat treatment of steel. Hence the measurement hardware should be capable of producing and operating reliably in temperatures around 1000°C. A custom heating stage could be added to almost any imaging method chosen, but conveniently, purpose built heating stages have already been developed for scanning electron microscope, which is utilised in this experiment.

Lastly it should be mentioned that there are numerous computational methods, ranging from thermodynamic to quantum mechanical models, that can be utilised to support the data analysis and/or predict the formation and behaviour of NMIs.

3 Scanning electron microscopy

Electron microscopes come in a variety of different forms, each tailored for a specific use case. The common principle among all of these instruments however is the same: An electron beam is generated by an electron gun and focused to a very small area on the specimen. Then the desired signal (electrons, x-rays, light etc.) is measured and an image or a spectrum is formed.

In scope of this thesis, we are dealing with bulk steel samples, which can be machined to expose any points of interest. Thus the scanning electron microscope (SEM) is best suited for this purpose. As the name suggests, SEM forms the image by scanning the electron beam across the sample area and a signal is measured in predetermined number of points resulting in a image consisting of pixels. [1]

3.1 Interaction mechanisms between sample and the electron beam

As the image in SEM is based on high speed electrons interacting with the sample material, it is vital to know what reactions can take place inside the sample and what signals can be measured from it. When the electron beam generated by the microscope hits the sample, a number of signals are generated. These different signals are shown in Figure 1 below.

Out of these signals the most useful ones are back-scattered electrons (BSE), secondary electrons (SE) and characterstic x-rays. Back-scattered electrons are, as the name suggests, primary electrons (from the beam) that through multiple elastic scatterings inside the sample material, change their trajectory enough to leave the sample. Secondary electrons and characteristic x-rays are the result of inelastic scattering of primary electrons. In inelastic scattering a primary electron excites an atom in the sample material. This excitation can relax either by ejecting an auger electron (secondary electron) or by releasing an x-ray, with energy that is characteristic to the element in question. It should be noted that secondary electrons can scatter further exciting more atoms and thus creating more secondary electrons. [1]
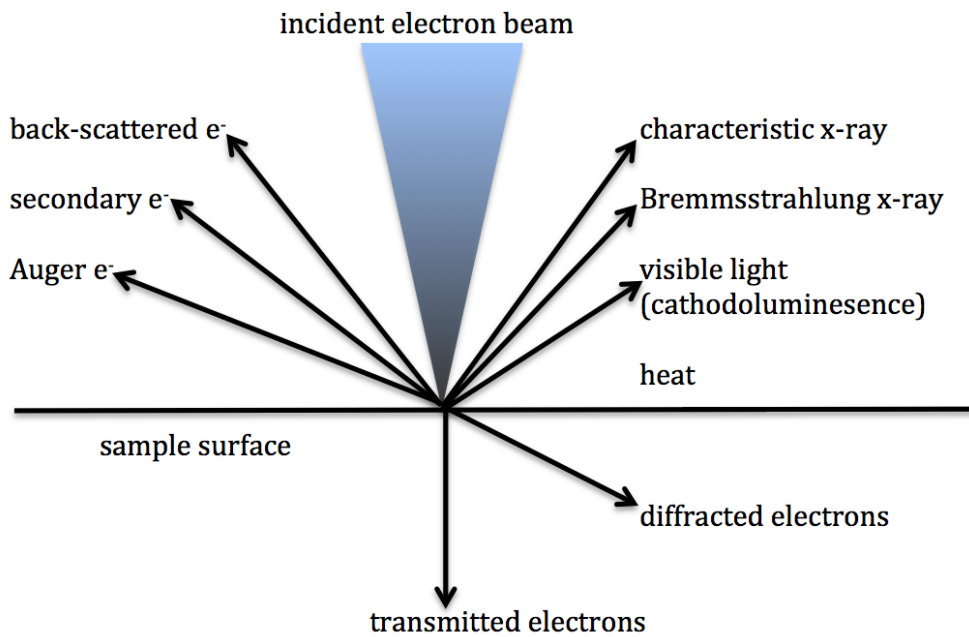

Figure 1: Possible interactions between sample and incident electron beam.

Image: Wyatt Tyrone Smith, https://en.wikipedia.org/ (CC BY-SA 4.0)

3.2 Image forming and interaction volume

Using the aforementioned signals, an image can be formed by focusing the electron beam to a very small area on the sample surface and measuring all the wanted signals from that point. Then the beam is moved and this point analysis is repeated until enough surface area has been covered. Image can now be formed by representing each analysed point as a pixel with a brightness corresponding to the signal strength at the point in question. Electron yield at a single point in the sample is dependent on the material and angle of the surface. Thus SEM images gives a good overview of the structure of the surface like a normal photograph would. Similarly images based on characteristic x-rays can be formed by presenting each element with different colour. An example of this so called EDS (energy dispersive spectroscopy) map can be seen in Figure 4. [1]

Although the word point is used, a signal in SEM always hails from larger area than the beam is focused on. This is simply due to the electrons scattering and spreading out inside

the sample. If an electron reaches certain depth, it cannot escape the sample and only way for it to contribute to the measurement is to excite an x-ray, which penetrates matter a lot easier. This spreading out and limit in depth results in interaction volume, which means the volume inside the sample from which a given signal can reach the detector of the microscope (see Figure 2). This is a major limiting factor in SEMs maximum resolution and has to be taken in account especially when interpreting EDS maps. [1]
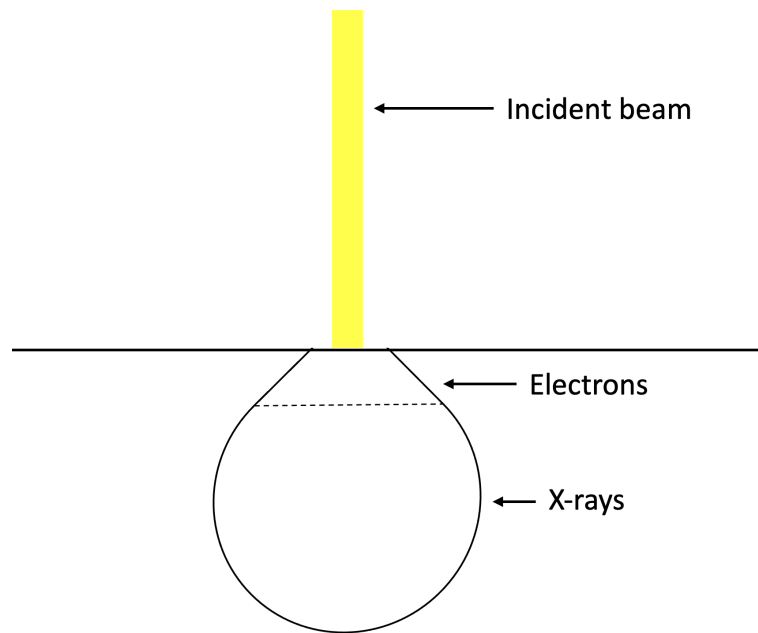

Figure 2: Interaction volumes of electrons and x-rays. x-rays reaching the detector hail from much larger volume resulting in reduced resolution. Typically the smallest attainable interaction volume for x-rays is around 1 μm^3 [1]

3.3   Components and structure of SEM

Since the focus of this particular thesis is in data analysis, different hardware configurations of SEM and working principles of individual components are not discussed in detail. Instead a brief overview of typical component types will suffice.

In order to generate a beam of electrons, an electron gun of thermal or field emission type is used. Thermal guns are simply filaments that release electrons when heated by electric current. Field emission gun is used when high beam currents are desirable. It consists of a very thin tip, which is placed in a strong electric field, where electrons are extracted from the tip by tunnelling effect. Most modern SEMs are equipped with field emission guns as they provide superior resolution when compared to their thermal counterparts. After being generated, the electrons are accelerated over high voltage to form a beam. Next the beam needs to be focused to a very small area on the sample. This is achieved using electromagnetic lenses. These lenses create magnetic fields, through which the electrons fly, and hence deflect the electron beam. By modifying the magnetic field, an effect similar to optical lenses is achieved. In addition to lenses, a number of apertures may be used to limit the beam size and trim away stray electrons. [1]

The above holds true for most electron microscopes, but for SEM one more component

needs to be added before the beam is ready to hit the sample. In a scanning type electron microscope, the electron beam needs to be moved over the sample surface by scan coils. These work in a similar fashion to the lenses except a coil is used instead of an electromagnet. Again, by modifying the magnetic field of the coil, electrons can be deflected resulting in the movement of the beam. Now the beam is focused and can be scanned over the sample area to obtain desired signals. [1]

Lastly, a detector is needed to measure the wanted signal. For electrons (SE and BSE), the two main types of detectors are scintillator and solid state detectors. In scintillator detector, the electron hits a scintillator material and a photon is emitted. These photons are then turned into an electric signal in a photomultiplier. In solid state detector, electron strikes a semiconductor and a number of electron-hole pairs is created. Normally these pairs would quickly recombine, but by applying a voltage (e.g. bias voltage of a P-N junction) the pairs may be separated resulting in a signal current. For x-rays, a similar detector to the solid state detector can be used. This energy dispersive spectrometer (EDS) measures the current created by x-rays producing electron-hole pairs in a semiconducting material. For better resolution and detection of lighter elements ($Z < 11$) a wavelength dispersive spectrometer (WDS) can be used. WDS however can only measure single wavelength at the time and is bigger and more complicated instrument than EDS, making it less practical for quick qualitative measurements. [1]
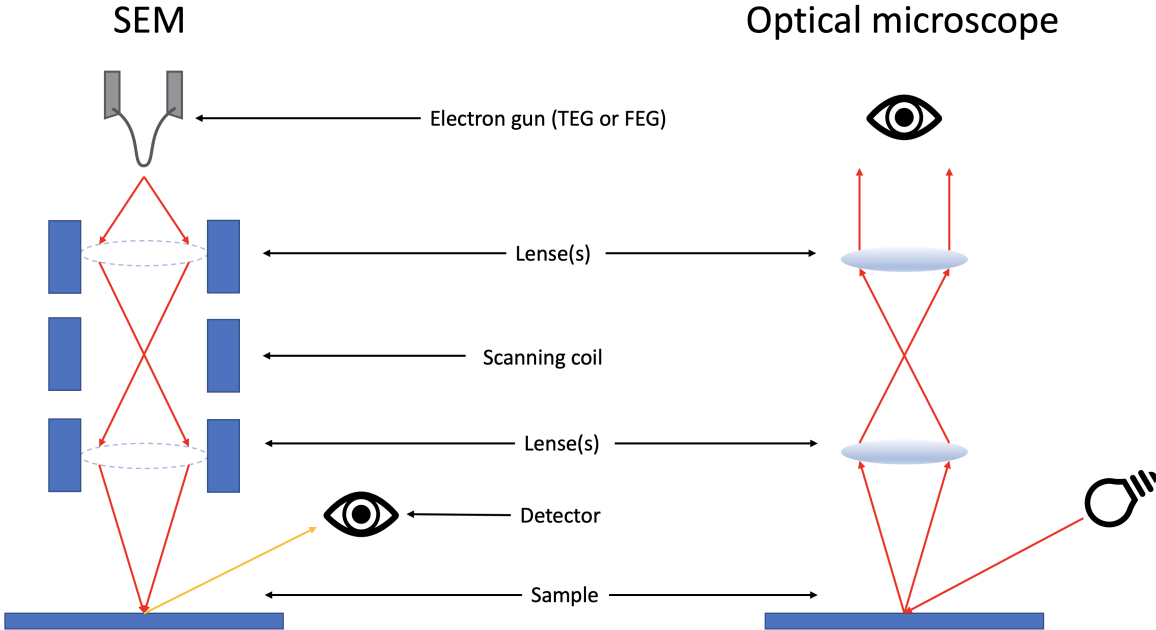

Figure 3: A simplified comparison between SEM and a typical optical microscope. We can see that the SEM actually works in a very similar fashion to the traditional microscopes, the biggest difference being the use of "electron compatible" components instead of normal lenses, light sources etc.

3.4 Limitations and future developement of SEM

The working principles of SEM set certain limitations as to what samples can be examined. The first and most fundamental restriction come from electrons needing a vacuum to travel any meaningful distance. Hence a vacuum (typically $< 10^{-4}$ pa) needs to be held inside of a conventional SEM and any sample unstable in low pressures is unsuitable for analysis. The most obvious ones being gases, liquids and most biological samples as they tend to contain water. [1]

Second significant limit is the conductivity of the sample. Since it is being bombarded with electrons, those electrons also need a way out of the sample. Otherwise a build-up of electrons could damage the sample or at least cause issues for image quality. In practice this means that the sample needs to be a conductor, which would limit the use of electron microscopy mostly to metallic materials. This limitation can fortunately be avoided by coating the sample with very thin layer of metal (e.g. gold, platinum...) or more commonly carbon. It has to be kept in mind though, that any thickness of coating will mask finer details from pictures and that the coating material will appear in x-ray spectra. Thus the coating should only be as thick as is needed to achieve sufficient level of conductivity. [1]

Third, the sample has to withstand the electron beam itself without deteriorating and lastly, the sample needs to be small enough to fit inside the microscope. This of course will depend on the specific model of microscope used, but generally samples smaller than 10 cm can be analysed. [1]

It should be mentioned that many methods have been developed to cope with previously mentioned limitations. These include but are not limited to freezing samples to analyse liquids, varying the pressure inside the microscope to allow samples requiring higher pressures to be analysed and limiting the accelerating voltage of the beam to analyse reactive samples [1]. Microscopes equipped with these capabilities are generally referred as environmental scanning electron microscopes (ESEM). The microscope used in acquiring the data presented in this thesis was actually an ESEM and hence is also capable of analysing wet samples or performing measurements in higher pressures (up to 750 pa). But as mentioned before, this is not important for steel samples.

3.5 High temperature SEM

The data in this thesis was produced with an ESEM equipped with a heating stage (hot stage). Heating stage allows the heating (and cooling) of the sample while inside the microscope. This in return makes it possible to analyse the sample in different temperatures from room temperature to around 1300°C. Important for this experiment, the temperature of the sample can be held constant over long time periods and measurements (pictures) can be taken at any time to monitor and record the state of the sample over time.

Before the experimental, let's go over some of the challenges faced when designing a heating stage for microscope and what limits they set for a high temperature SEM (HT-SEM). First and the most obvious one is over heating of components. In order to prevent this, heat shields need to be installed between the sample holder/heater and rest of the microscope and in case of more extreme temperatures, a cooling system to be added to the heating stage. Heat also affect the microscopes ability to image as a standard semiconductor backscattered electron detector doesn't work well with black body radiation coming from a hot sample. Fortunately heat resistant BSE detectors have been developed, which allow BSE

imaging up to 1050°C [8]. In higher temperatures HT-SEM is limited to using secondary electrons. [10]

In addition to black body radiation, a hot sample and especially the heating element itself also emits thermal electrons. These electrons have to be separated from the secondary electrons used for imaging. Otherwise they will significantly worsen the image quality. Again, carefully placed heat shielding can be used and heating stage materials chosen to minimize thermal electron yield at the detector. The detector still needs to be reached by secondary electrons an so in order to completely get rid of thermal electrons, they need to be filtered out. This can be done by a suppression grid bias so that it lets the higher energy secondary electrons pass, but captures low energy thermal electrons.[10]

There are a few ways to heat the sample. The most common heating solution is to use a filament or a boat that is heated by electric current. A sample can be placed in contact with this heating element or the element can be wound around the sample to form a kind of oven. Temperatures up to 2500°C may be reached depending on the implementation. Second way of heating is by using a laser (LASEM). A laser beam is simply directed at the sample surface to heat it. This method creates steep temperature gradients and temperatures up to 1700°C on the sample surface, which may be either advantageous or disadvantageous depending on the study it is used for.[10]

Lastly the temperature of the sample surface has to be able to be measured as accurately as possible. In order to do this, a thermocouple can be placed in direct contact with or very close to the sample. Alternatively an optical pyrometer or an infra-red camera can be used. The latter can also be used to map the temperature gradient across the sample surface.[10]

1. Electron detector
2. Electron beam
3. Heat shield
4. Hot filament
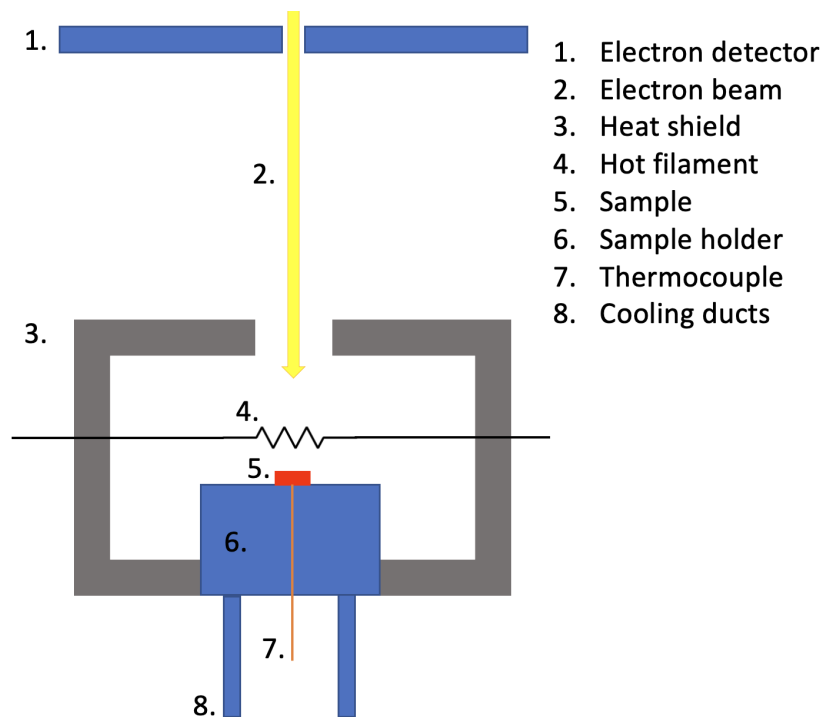5. Sample
6. Sample holder
7. Thermocouple
8. Cooling ducts

Figure 4: Simplified heating stage for SEM. Heat shield provides thermal insulation and reduces thermal electron emission. Heating is provided by a filament and sample temperature is measured by a thermocouple placed in direct contact with the sample.

4 Methods

The data analyzed for this thesis is part of research carried out at University of Oulu, Nano and molecular systems research unit and process metallurgy research unit [4]. The objective of this experiment is to see if there are any noticeable changes in either size or shape of multicomponent inclusions and if there is any diffusion between NMIs and the steel matrix during heat treatment at temperatures around 800-900 °C. At the same time it will be evaluated if the hot stage SEM even is suitable for analysing inlcusions in steel. Similar research has been carried out before, focusing on bearing steels [8]. In these experiments, the samples were anlaysed before and after treatment only. Hot stage in-situ NMI experiments like this one have not been performed before. CSLM (confocal scanning laser microscopy) has been utilised in similar experiments, though without the in-situ aspect [6].

Table 1: Table of all analysed inclusions.

Inclusion	type
A1	CaS
A2	CaS + Al_2MgO_4
A3	CaS + Al_2MgO_4
A4	CaS
A5	TiN
A6	MgS
R1	Al_2MgO_4
R2	CaS + Al_2MgO_4
R3	MnS
R4	CaS + Al_2MgO_4
R5	CaS + Al_2MgO_4
R6	Calsium aluminates + CaS
R7	CaS + Al_2MgO_4
R8	TiN
R9	CaS + Al_2MgO_4
R14	TiN
R15	CaS
R16	CaS
R17	CaS + Al_2MgO_4
R18	CaS + Al_2MgO_4
R19	CaS
R20	CaS
R21	CaS + Al_2MgO_4

The samples used in this experiment are low-alloyed carbon steel, aluminum-killed and calcium treated. The samples are from different heats of hot rolled steel. In order to prepare the samples for Hot stage SEM, they were first cut down to appropriate size (thin disks of around 5 mm in diameter) and then polished. Then all the exposed inclusions were analysed by conventional SEM and interesting NMIs were selected for analysis and labelled before sending the samples for the hot stage SEM.

In the HT-SEM, samples were then heated to either 800 °C or 900 °C and kept at that temperature for 30 - 120 minutes before being cooled back down to room temperature (fig. 5). Chemical composition of the inclusions in samples was recorded using SEM-EDS before and after experiment. SE/BSE pictures were also taken during the experiment to observe possible changes in greater temporal detail. List of analysed samples is provided in Table 1.
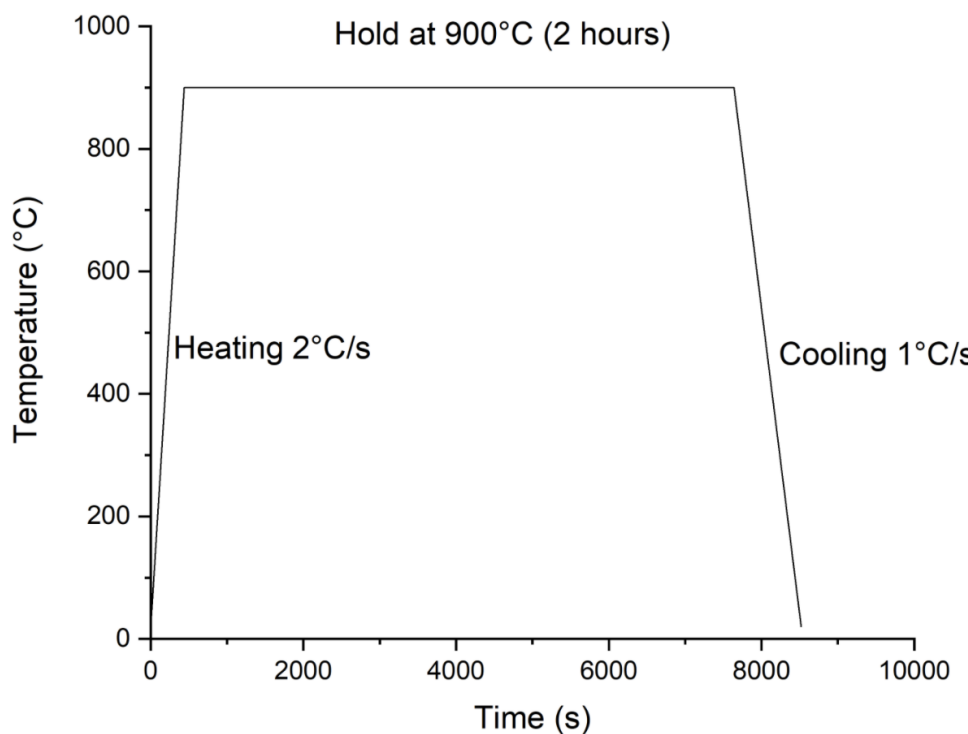

Figure 5: Example of temperature profile during the experiment.

Afterwards, EDS maps taken before and after heat treatment were compared against each other and differences between them were recorded. Time lapse videos were also compiled from SE/BSE pictures taken during experiment and used to confirm findings in EDS comparison.

From this inital analysis, interesting inclusions were further analysed using line scans and further research was done regarding the reasons behind observed reactions. However this thesis is only focused on the initial analysis described above and thus is limited to only identifying the general trends among the sample inclusions and evaluating the usefulness of hot stage SEM in investigation of inclusions.

5 Results and discussion

5.1 Results

The inclusions in this data could be divided to two broad categories: Inclusions consisting of only one component and inclusions containing multiple phases. In terms of chemical composition, typical phases in the analysed inclusions were CaS, Al_2MgO_4, TiN and MnS, as noted in Table 1. Small amounts of other phases were also present but their contribution to either the size of the inclusions or the results was negligible in all cases.

In inclusions containing multiple components, typically at least CaS and Al_2MgO_4, a recurring pattern of small amounts of CaS dissolving into the steel matrix was observed. More specifically, "pits" formed to parts of the inclusion containing CaS and EDS maps taken after the experiment showed that these "pits" were "filled" by Fe, as if the surrounding steel had carved away part of CaS (see Figures 6 and 7 below). In some inclusions small Fe droplets formed inside the CaS phase in a similar fashion to the pits mentioned above. Magnesium aluminate phases in these inclusions didn't undergo any visible changes.

Inclusions consisting of only one component (mainly TiN) generally didn't show any changes during treatment. TiN specifically remained unchanged in all the inclusions examined. Some single component CaS and MnS inclusions however exhibited the dissolving process described above.

In some inclusions regardless of their composition, voids formed around the inclusion during the heating process(see Figure 10). This is probably due to phase changes in the surrounding steel matrix rather than in the inclusion itself. It has been shown that steel expands in austenite to ferrite transformation [7] and it seems to be reasonable to assume that here a reverse phenomenon takes place as steel transforms from ferrite to austenite. It should be also taken into account that at temperatures of around 800-900°C some of the inclusion materials as well as the surrounding steel starts to soften which can promote this formation of voids, and all the other observed phenomena for that matter.

Figure 6 below demonstrates the aforementioned dissolving of CaS in multicomponent inclusions by comparing the EDS-maps (refered to just maps from here on out). The inclusion (R18) consists mainly of CaS, with some magnesium aluminate. The aluminate phase remains unchanged, but the CaS phase visibly shrinks during treatment. When comparing to Fe-map it can be seen that areas previously occupied by CaS have been filled out with Fe. As the surface of the inclusion is exposed, it is technically possible that some steel has simply covered parts of the inclusion, but this seems unlikely to be the case for all the inclusions examined.
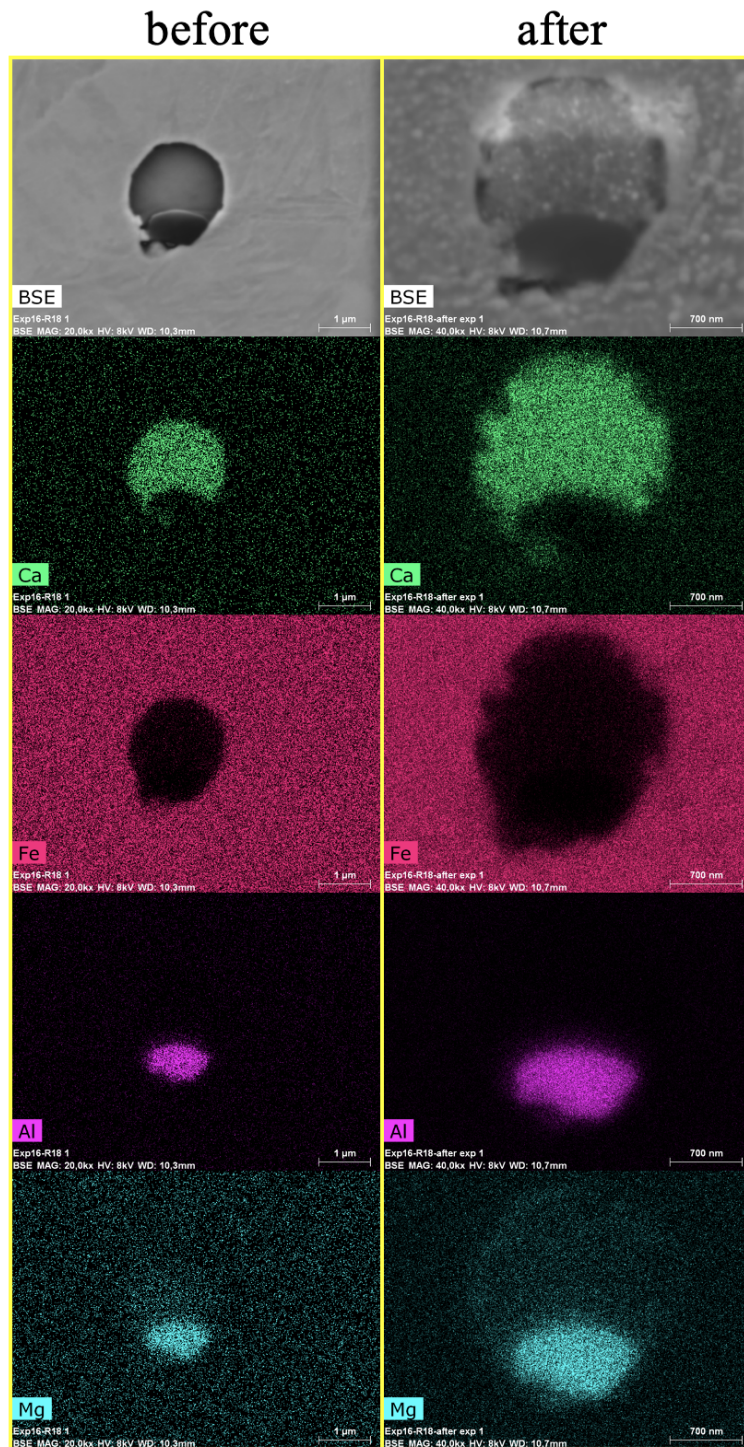
Figure 6: Typical example of CaS dissolving into surrounding steel. Pictures above are taken before the experiment and below ones are after. BSE picture shows the whole inclusion.

Figure 7 shows a single component CaS inclusion (R19) undergoing the same dissolving phenomenon. On Figure 8 is a similar single component CaS inclusion (R20) that remains effectively unchanged. Next to R20 there are large voids or recesses which might prevent any interaction taking place. On the other hand, the bottom left hand side of the inclusion should be free to interact. EDS maps also show notable amount of silicon present in the recesses. This is simply residue from the polishing process, which utilises silicon based polish. This residue is also present on most other inclusions.
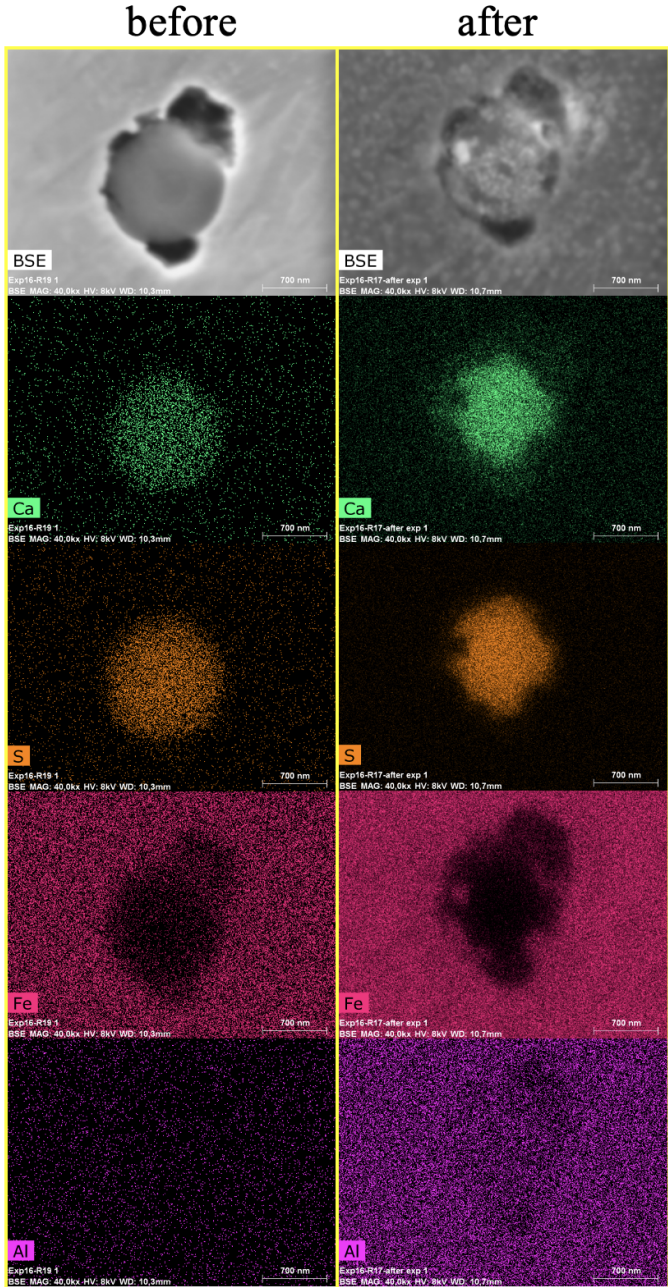

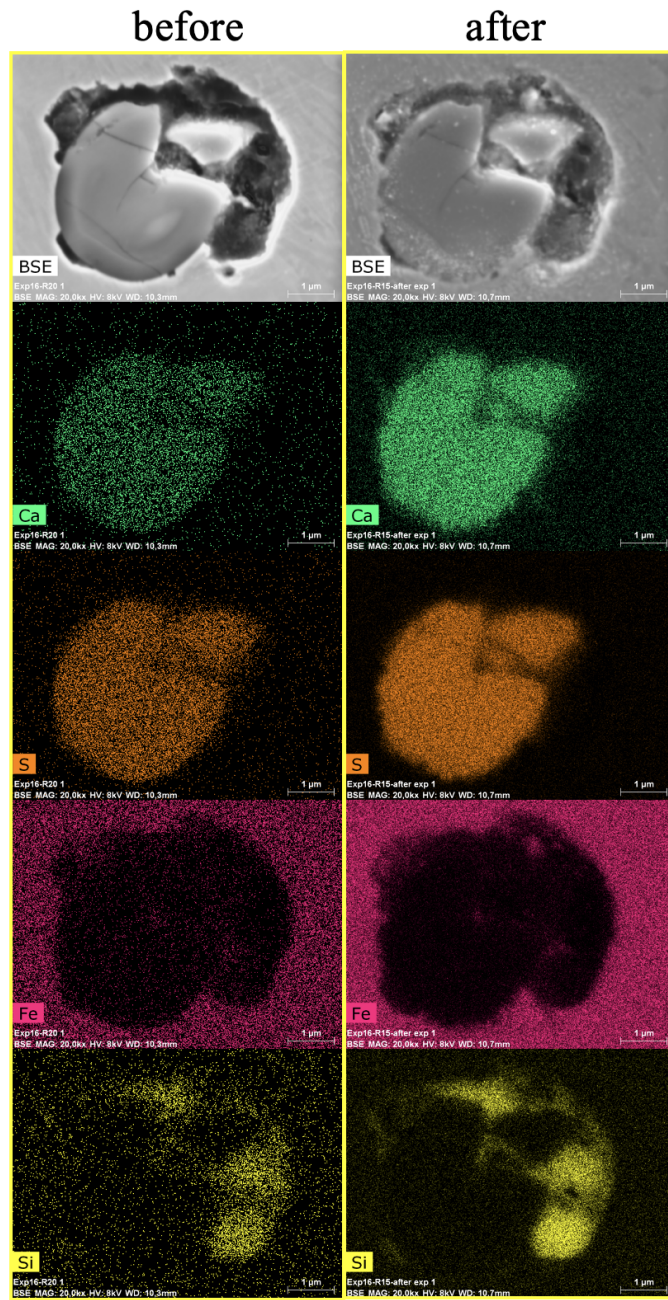Figure 7: Single component CaS inclusion with visible dissolving

Figure 8: Single component CaS inclusion that remains unchanged. Recesses around inclusion contain remains of silicon based polish.

Inclusion (R6) in Figure 10 contains some calsium aluminate phases in addition to magnesium aluminate. This calcium aluminate doesn't seem change like CaS does. Only visible changes in the inclusion happen to the "tail" of the inclusion, which seems to expand a little. However it is difficult to judge what exactly causes this. As the potential calcium aluminate phases were deemed interesting, further analysis was performed for this inclusion. Attached below is a table of point analysis data. It shows atomic percentages of different elements in selected points of the inclusion (Figure 9).
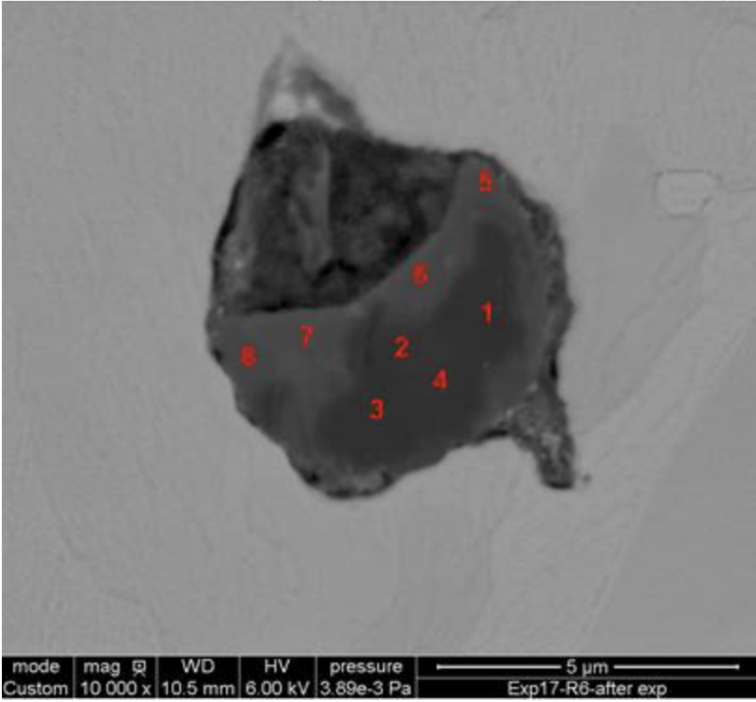

Figure 9: Points of analysis.

Spectrum	O (at%)	Mg (at%)	Al (at%)	Si (at%)	P (at%)	Ca (at%)
Exp17-R6-after exp 1	57,30226	13,46721	28,69367	0,091306	0,110923	0,334627
Exp17-R6-after exp 2	57,20305	13,61696	28,56435	0,086872	0,024702	0,504057
Exp17-R6-after exp 3	57,22812	13,69874	28,6935	0,024546	0,056635	0,298455
Exp17-R6-after exp 4	57,27495	13,6348	28,60074	0,100091	0,09963	0,289786
Exp17-R6-after exp 5	57,33812	0,576432	27,02985	1,048175	0,075431	13,93199
Exp17-R6-after exp 6	56,828	0,18195	26,89723	0,138806	0,04572	15,90829
Exp17-R6-after exp 7	56,59716	0,585577	25,35673	0,456235	0,03982	16,96447
Exp17-R6-after exp 8	56,6896	0,094246	26,54521	0,00193	0,069771	16,59924

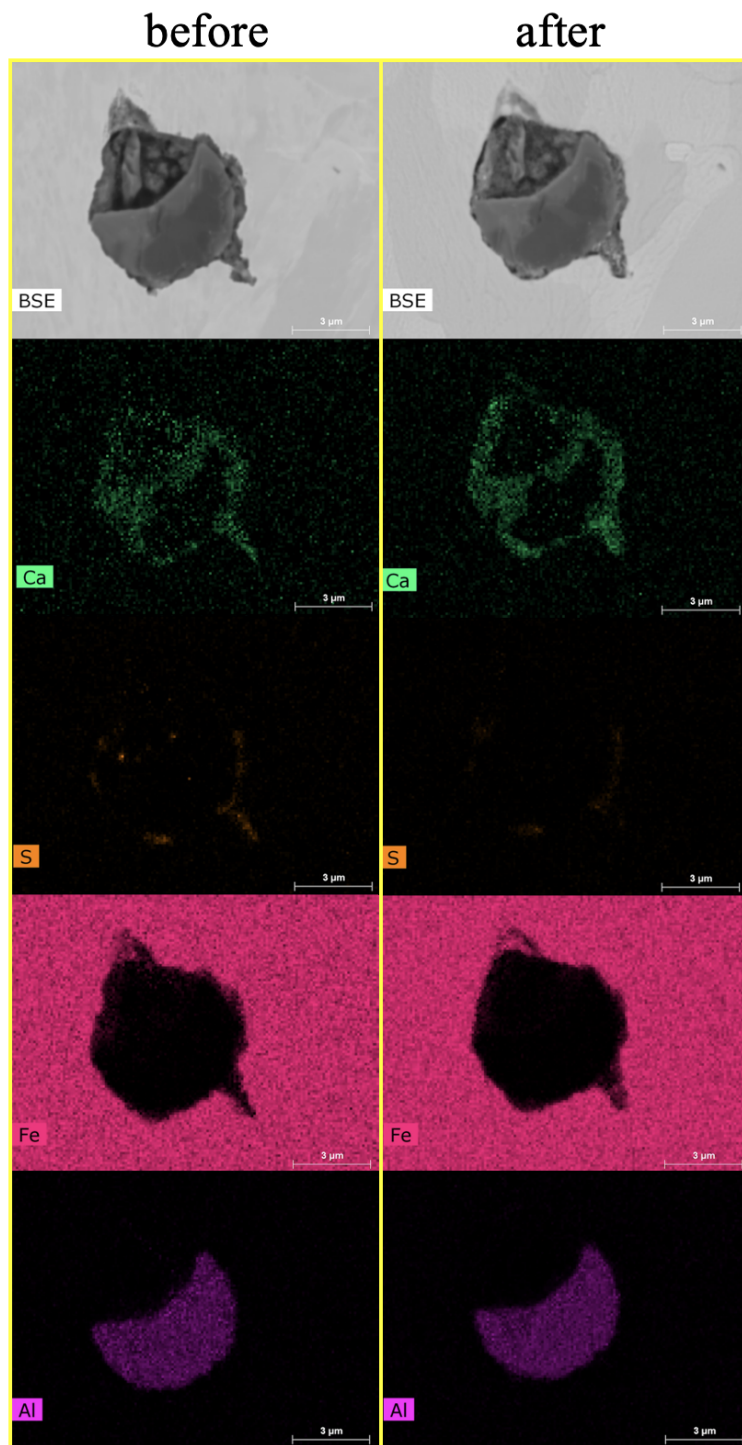Table 2: Table of atomic percentages at different points in inclusion R6.

Figure 10: Multicopmponent inclusion containing some calsium aluminate phases.

Figure 11 shows a single component TiN inclusion. As mentioned previously, TiN inclusions or TiN parts of multicomponent inclusions did not interact with the steel matrix in any visible way.
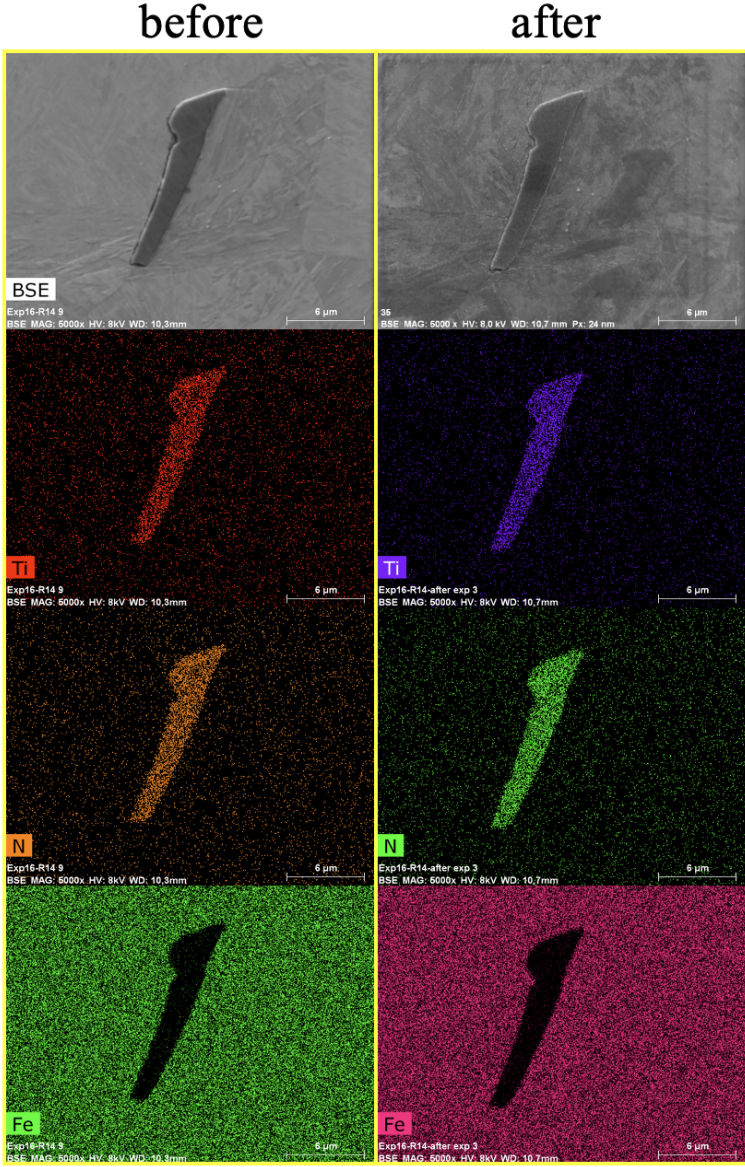

Figure 11: TiN inclusion showing no visible interaction with surrounding steel matrix.

Lastly Figure 12 shows a single component MnS inclusion (R3). On top right hand corner of the inclusion, some MnS seems to dissolve in to the steel matrix in a similar fashion to CaS described earlier. BSE pictures show black voids forming at the interface between the inclusion and the steel matrix. This is propably due to phase changes in the steel mentioned above. When the right edge of the inclusion is examined, it can be seen that that voids prevent the interaction between inclusion and steel as they are not physically in contact with each other.
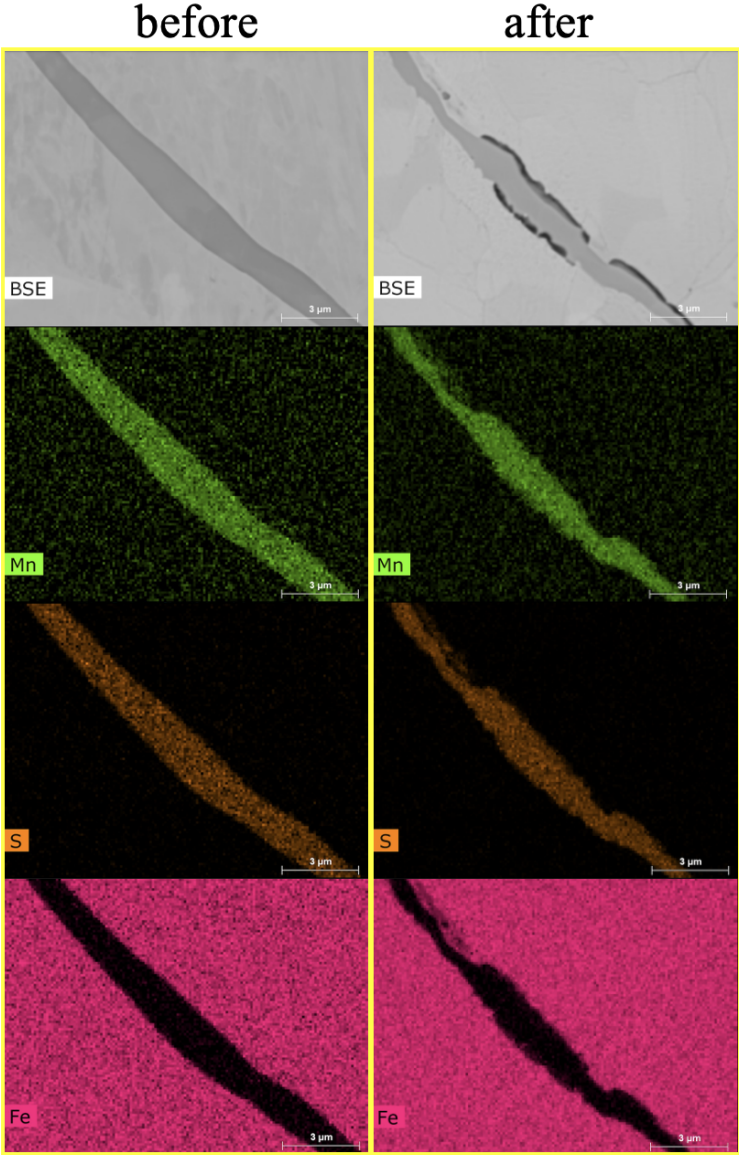

Figure 12: MnS inclusion showing some dissolvation to surrounding steel matrix. In BSE pictures voids (black) appear at inclusion-steel interface

5.2   Discussion

On surface level, high temperature in situ SEM seems to be suitable method in examining inclusions in steel. However there are few caveats that should be taken into consideration when doing this kind of experiments. Firstly, the samples in this experiments were machined and polished to expose the inclusions. While this doesn't seems to affect the results in any obvious way apart from silicon residue in some inclusions, it is possible that inclusions would behave slightly different if they were completely inside the steel matrix. Of course the pre treatment analysis of inclusions can not be done, if this approach is taken. At least not with SEM. Second, lack of full topographical data and the generally soft resolution of pictures makes it difficult to tell apart actual reactions between phases and effects that result from changes in vertical plane (see results section: inclusion R18).

Temperature range of this particular hot stage SEM is large enough to observe steel in any realistic treatment temperature. A follow-up study could be done to confirm this assumption. In terms of holding temperatures used in this study, the results seem twofold. On the other hand, somewhat unexpected reactions were observed in CaS-type inclusions, which could prove to be useful in the future. However, the cracks and voids between the inclusion and the steel matrix formed by phase changes in the steel itself prevents any interactions between the two. In the end this did not prove to be detrimental as some inclusions or parts of some inclusions were not affected, but this should be taken into account if similar studies are carried out in the future.

Finally, the resolution and accuracy of imaging with SE and analysis with EDS is fine when identifying bigger changes within the whole inclusion, like has been done here. But for more in depth or local analysis the limits of EDS start to show. Line scans and point measurements were also performed for potentially interesting inclusions after initial hot stage measurements. These were not analysed in this thesis not only in order to keep the length in check, but also partially because the data acquired did not reveal anything new or give better insight to phenomena already observed with other methods.

6   Conclusions

In summary, hot stage scanning electron microscope was found to be a suitable method for carrying out relatively quick and generalized analysis of non metallic inclusions in steel. Poor resolution and accuracy of EDS, lack of proper depth information and the fact that inclusions have to be exposed limit it's capabilities in more thorough local analysis of inclusions or parts of them. In terms of inclusions analysed in this thesis, it was found that CaS has a tendency to dissolve in to the surrounding steel matrix in multicomponent inclusions at temperatures around 900°C. Some dissolving was also visible in couple of single component CaS and MnS inclusions. Phase changes in surrounding steel matrix were noted to partially prevent any interaction between inclusions and surrounding steel.

7   Acknowledgements

8 References

[1] Goodhew, P. J., Humphreys, J. & Beanland, R. (2001). Electron microscopy and analysis (3. ed.). Taylor & Francis.

[2] A.B. Schmiedt, H.H. Dickert, W. Bleck, U. Kamps, Acta Mater. 95 (2015) 1–9.

[3] Y. Wang, A. Karasev, P.G. Jönsson, Steel Res. Int. 91 (2020) 1900669.

[4] Singh, H., Alatarvas, T., Kistanov, A. A., Assa Aravindh, S. D., Wang, S., Zhu, L., . . . Fabritius, T. Unveiling interactions of non-metallic inclusions within advanced ultra-high-strength steel: A spectro-microscopic determination and first-principles elucidation. Elsevier.

[5] Ekta Rani, Harishchandra Singh, Tuomas Alatarvas, Mourad Kharbach, Wei Cao, ... Uncovering temperature-tempted coordination of inclusions within ultra-high-strength-steel via in-situ spectro-microscopy, Journal of Materials Research and Technology, Volume 17, 2022, Pages 2333-2342

[6] Wang, Q., Zou, X., Matsuura, H. et al. Evolution of Inclusions During the 1473 K (1200 °C) Heating Process of EH36 Shipbuilding Steel. Metall Mater Trans B 49, 18–22 (2018).

[7] Battle, T., Eric, H., Holappa, L., Jalkanen, H., Kitamura, S., Louhenkilpi, S., Madias, J., Mills, K., Raipala, K., Wijk,...(2014). Treatise on Process Metallurgy, Vol 3: Industrial Processes: Part A Ferrous Process Metallurgy. Elsevier.

[8] Cheng, Gong & Li, Weifu & Zhang, Xianguang & Zhang, Lifeng. (2019). Transformation of Inclusions in Solid GCr15 Bearing Steels During Heat Treatment. Metals. 9. 642. 10.3390/met9060642.

[9] Podor R, Mendonça J, Lautru J, et al. Evaluation and application of a new scintillator-based heat-resistant back-scattered electron detector during heat treatment in the scanning electron microscope. Journal of Microscopy. 2020;1-15.

[10] R. Podor, G.I. Nkou Bouala, J. Ravaux, J. Lautru, N. Clavier, Working with the ESEM at high temperature, Materials Characterization, Volume 151, 2019, Pages 15-26